CYCLOTRON WAVE INSTABILITY IN THE CORONA AND ORIGIN OF SOLAR RADIO EMISSION WITH FINE STRUCTURE

III. *Origin of Zebra-Pattern*

V. V. ZHELEZNYAKOV and E. YA. ZLOTNIK
Radiophysical Research Institute, Gorki, U.S.S.R.

(Received 24 October, 1974; revised 4 April, 1975)

Abstract. The results of investigation of the cyclotron wave instability in the corona for Bernstein modes and plasma waves in a hybrid band have been used to interpret zebra-pattern phenomena. Two models of the generation region of parallel drifting bands are considered: the model of the point source localized at the apex of the magnetic trap and the model of a distributed source extended along the magnetic flux tube. In the first model it is assumed that a harmonic character of zebra-pattern appears either in coalescence of excited Bernstein modes at different harmonics of the gyrofrequency or in coalescence of these modes with plasma waves excited in the hybrid band. In the latter case if the magnetic field changes in time a pulsating generation regime occurs. In the second model, the emission bands appear in the regions of double plasma resonance as a result of coalescence of longitudinal waves excited in the hybrid band. Estimations of the magnetic field and the nonequilibrium component density necessary for the zebra-pattern to generate are presented.

1. Introduction

This part deals with interpretation of zebra-pattern of the solar radio emission, the example of which in the event of 2 March 1970 is illustrated on the dynamic spectrum of Figure II.1a*. The figure shows the period followed by the appearance of 'tadpoles', zebra-pattern at this time consisting of tadpoles almost overlapped. In many other events, however, zebra-structure was recorded as continuous bands (see, for example, Slottje (1972a)). Due to this Slottje (1972a) concluded that there were two different kinds of zebra-structure: related and not related with tadpoles.

We may point out two models of generation of parallel drifting bands (zebra-structure): the model of a 'point' source localized at the apex of the magnetic trap (see Figure II.2) and the model of a 'distributed source' extended along the magnetic flux tube. For the first model, the generation region dimensions are assumed to be so small that the magnetic field and plasma density inhomogeneity has no influence on the frequency spectrum. In the second model, it is just the change in the magnetic field and coronal plasma density along the flux tube that plays the main role.

In both models it is taken into account that the emission bands in zebra-pattern

* Here and below a roman II before the number of the formula or figure denotes a reference to the corresponding formula or figure in the paper by Zheleznyakov and Zlotnik (1975b) cited as II. A roman I refers to the paper by Zheleznyakov and Zlotnik (1975a).

Solar Physics **44** (1975) 461–470.

are separated by approximately equal frequency intervals. This points to the association of zebra-structure (and tadpoles arising as zebra-structure development and continuation in the event on 2 March 1970) with emission at the harmonics of the electron gyrofrequency Ω_H.

2. Origin of Zebra-Structure Emission in the Event on 2 March 1970

It was shown in Part II that the tadpole generation on 2 March 1970 may take place in the small source where Bernstein modes are excited. To explain the zebra-structure closely related with tadpoles during the event, we use the model of the point source localized at the apex of the magnetic trap (Figure II.2).

The energetic particle distribution in the source is defined by formula (II.3.1).

It should be emphasized that a 'banded' dynamic spectrum in such a model may be caused by two different ways. The first generation scheme (II.2.1.) was discussed in Part II. Bernstein modes are generated in the source; the radio emission is generated in coalescence of these modes with different or equal numbers of harmonics s_1 and s_2. The radio emission frequency is

$$\omega_r \sim s_1\Omega_H + s_2\Omega_H. \tag{2.1}$$

The second way is also based on excitation of Bernstein modes at relatively small harmonic numbers $s\Omega_H$ ($s<10$). The combination scattering (coalescence) of these waves with plasma waves excited in the hybrid band (near the frequency $\Omega_h \simeq \Omega_p = (4\pi e^2 N_0/m_e)^{1/2}$*) gives rise to electromagnetic radiation recorded as zebra–pattern (the generation scheme by Rosenberg, 1972). The radio emission frequency may be represented as

$$\omega_r \approx \Omega_p + s\Omega_H \tag{2.2}$$

bearing in mind that the excited Bernstein mode frequency and the plasma wave frequency may essentially differ from Ω_H and Ω_p (in the value smaller or comparable with Ω_H).

The minimum frequency of emission which escapes the local source and reaches the Earth is $\omega_{\min} \approx \Omega_p$. The intervals between bands $\Delta\omega \approx \Omega_H$, the frequency band drift is caused by the temporal change in Ω_p or Ω_H (i.e. the coronal plasma density and the magnetic field intensity) in the generation region.

After the preliminary remarks have been made, we proceed to direct explanation of zebra-structure observed on 2 March 1970.

The appearance of almost continuous harmonic bands on the spectra in Figure II.1a (instead of well differentiated tadpoles in Figure II.1b) testifies to the fact that the energetic particle injection into the source was quasi-continuous. Some discontinuity turned to be sufficient for Slottje to make a conclusion on the genetic relation between zebra-pattern and tadpoles, the latters being the members of zebra-pattern.

* This equality as well as the formula (2.2) are given under the assumption that $\Omega_H \ll \Omega_p$.

This circumstance is a strong argument in favour of the common generation mechanism for both types of the fine structure in the event under consideration. Therefore in accordance with the conclusions made in Part II we assume that the zebra-pattern is also caused by the cyclotron Bernstein mode instability with a subsequent coalescence of excited modes into the electromagnetic radiation (see (2.1)).

The distance between zebra-structure bands is of the order of Ω_H. If follows from Figure II.1a that the value $\Omega_H \sim 2\pi \times 15$ MHz ($H \sim 5$ Oe). The presence of a stable low-frequency boundary (nearly 200 MHz) in the zebra-pattern on the dynamic spectrum (Figure II.1a) is due to the condition $\omega_r > \Omega_p$ for radio emission escaping from the local source. From the inequality $\omega_r > \Omega_p$ we obtain at once the plasma wave frequency $\Omega_p \approx 2\pi \times 200$ MHz in zebra generation region. The ratio $\Omega_p/\Omega_H \approx 15$ and consequently the sum of harmonic numbers of coalescing Bernstein modes will be $s_1 + s_2 \gtrsim 15$.

From Figure II.1a it follows that the frequency drift rate in the zebra-structure is $\mathrm{d}\omega_r/\mathrm{d}t \sim 2\pi \times 10$ MHz s^{-1}. Since the value $\Omega_p = \text{const}$, the drift is caused by the change in the magnetic field in the source (see (2.2) and (2.1)). From formula (II.2.2) at $s_1 + s_2 \sim 20$ we obtain that during the zebra-pattern generation on 2 March 1970 the derivative $\mathrm{d}\Omega_H/\mathrm{d}t \sim 2\pi \times 1$ MHz s^{-1}. At this time the relative change in the gyrofrequency (or magnetic field) per unit time $(1/\Omega_H)\,\mathrm{d}\Omega_H/\mathrm{d}t \sim 1/15$ was approximately 4 times less than the corresponding value during tadpole generation (see Part II).

In the framework of the generation scheme (2.1), an excitation of longitudinal waves in the hybrid frequency band is not necessary for the zebra-pattern to occur. At the same time this is quite possible, as well as the Bernstein mode generation at the lower frequencies. Here it should be noted that at comparatively low velocities of hot electrons $v_e/v_T \sim 4$ providing, in particular, the developed tadpoles to appear (see Section 2), the longitudinal wave generation in the hybrid band has much in common with Bernstein mode generation at the lower frequencies. The latter is due to the fact that for small enough ratios v_e/v_T the instability in the hybrid band occurs in those parts of the dispersion curves $\lambda_{cr} > n$ the behaviour of which resembles the dependence $\omega(\lambda)$ for Bernstein modes (see Figure I.2a where, in particular, the kinematic instability boundary λ_{cr} is shown for $v_e/v_T = 4$). The generation conditions described are typical for zebra-structure in that part of the event on 2 March 1970 when the pulsating regime was absent.

The appearance of pulsations with the period 0.7 to 0.8 s on the dynamic spectrum (Figure II.1a) may be associated with the periodic occurrence of the double plasma resonance in the source if the particle velocities are rather great (for example, $v_e = 20 v_T$ during the whole pulsating regime). In this case the kinematic instability boundary λ_{cr} in the hybrid band in Figure I.2a moves leftwards ($\lambda_{cr} < n$) towards that interval of λ in which the behaviour of dispersion curves depends essentially on the ratio Ω_p/Ω_H. The generation efficiency increases sharply, at the same time it will be strongly varied with changing $\Omega_h/\Omega_H \approx \Omega_p/\Omega_H$, reaching the greatest values under the condition $n\Omega_H \approx \Omega_p$ (the double plasma resonance, see Figure I.6a, b). Due to the monotone temporal change of Ω_H the condition $n\Omega_H \approx \Omega_p$ is periodically realized at different

values of n, resulting in the pulsating regime with a periodic change of the intensity of plasma waves excited in the hybrid band. These waves, coalescing with excited Bernstein modes, yield the radio emission which is also of the pulsating character. This is clearly seen on the dynamic spectrum of the zebra-pattern in Figure II.1a.

In the pulsating regime, the generation scheme (2.1) becomes invalid. The most intensive radio emission generates at this time in accord with the scheme (2.2).

The pulsation period is apparently equal to the time τ during which the double plasma resonance condition $n\Omega_H(t) \approx \Omega_p$ is substituted by the condition $(n-1)\Omega_H \times \times \Omega_H(t+\tau) \approx \Omega$ (at $\Omega_p = \text{const}$ and $d\Omega_H/dt > 0$). Assuming that $\Omega_H(t+\tau) \approx \Omega_H(t) + + (d\Omega_H/dt)\tau$, we find

$$\tau \approx \frac{1}{n-1} \frac{\Omega_H}{d\Omega_H/dt}. \tag{2.3}$$

For $n = 15$, $\Omega_H \approx 2\pi \times 15$ MHz and $d\Omega_H/dt \sim 2\pi \times 1$ MHz s^{-1} we obtain $\tau \sim 1$ s that is close to the observed values of the pulsation period.

Thus the zebra-structure pulsating regime is caused by the enhanced generation of longitudinal waves during periodic appearance of doubleplasma resonance in the source with increasing magnetic field. The electromagnetic radiation occurs due to coalescence of Bernstein modes (kinematic instability) excited at the low harmonics of the gyrofrequency with intensive plasma waves in the hybrid band (relativistic and kinematic instability).

The probability of conversion of the longitudinal waves into electromagnetic radiation was investigated in the paper by Chiuderi *et al.* (1973). However the calculation made is not free of objections. The fact is that the intensity of the electromagnetic radiation was obtained with talking into account the compensation effects which decrease essentially the conversion efficiency. However when the waves with different frequencies (Bernstein modes and plasma waves in the hybrid band) interact, the compensation does not occur. A correct calculation of conversion is given elsewhere. Note that the radiation patterns are different for ordinary and extraordinary waves resulting from the nonlinear coalescence of Bernstein modes and plasma waves in the hybrid band. Due to this the zebra-pattern radio emission generated in the 'point' source may appear to be polarized.

Apart from the pulsation regime with a distinct period, there appear wedge-shaped broad-banded absorptions on the dynamic spectrum (Figure II.1a). They may be due to stopping of the cyclotron instability (plasma wave and Bernstein mode generation) at the time when the electron streams are injected into the source. The stream fills a 'gap' at small transverse pulses $p_\perp$ in the nonequilibrium distribution function (II.3.1) which provides the zebra-structure generation. This gap corresponds to the loss cone for the particles trapped by the magnetic field. The resulting particle (stream + electrons trapped) distribution becomes stable and the radio emission generation ceases until the stream particles leave the local source (Zaitsev and Stepanov, 1974, 1975).

3. Generation of Zebra-Structure not Related with Tadpoles

Some phenomena, belonging to this type of the fine structure are possibly generated under the conditions of the point source model. As an example, we refer to the dynamic spectra of zebra-pattern observed by Elgarøy (1961) which have an oscillating band drift. The latter may be due to periodic oscillations of the magnetic field in the source produced, for instance, by propagation of a magneto-hydrodynamic wave of the wavelength λ_m. The condition of observing such oscillations $L<\lambda_m$ imposes limitations on the source dimensions $L<2\times 10^7$ cm.

However we believe the situation to be more general when a banded dynamic spectrum appears in the model of the distributed source formed by nonequilibrium energetic particles which fill a magnetic flux tube (Figure 1). For the sake of simplicity, the velocity particle distribution is also assumed to be (II.3.1).

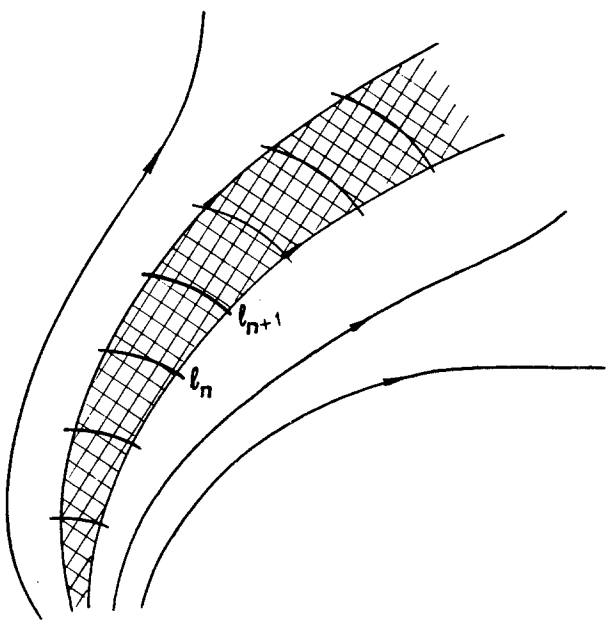

Fig. 1. Model of distributed source extended along the magnetic flux tube.

In this model the appearance of light bands is associated with a strong enhancement of plasma wave generation at double plasma resonance when the upper hybrid frequency is close to one of the harmonics of the electron gyrofrequency

$$\Omega_h \approx n\Omega_H . \tag{3.1}$$

If $\Omega_H \ll \Omega_p$, i.e. $\Omega_h \approx \Omega_p$, the double resonance condition has the form

$$\Omega_p(l) \approx n\Omega_H(l) \tag{3.2}$$

(l is the coordinate along the flux tube). The radio emission may occur due to coalescence of two excited plasma waves with the frequencies near Ω_p; the radio emission frequency is*

$$\omega_r \approx 2\Omega_p \approx 2n\Omega_H . \tag{3.3}$$

The appearance of parallel bands (zebra-pattern) in the distributed source model may be understood from Figure 2. It illustrates the distributions $\Omega_p(l)$ and $\Omega_H(l)$ along the flux tube. If the dependences $\Omega_p(l)$ and $\Omega_H(l)$ are different, the double resonance con-

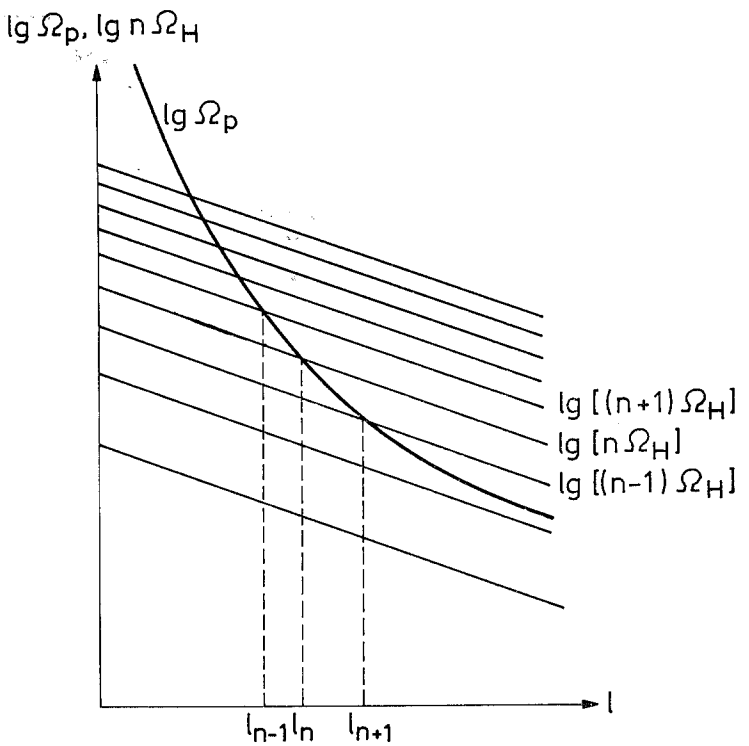

Fig. 2. Levels of double plasma resonance in the distributed source.

dition (3.2) is realized only for the chosen values of l_n satisfying the points of intersecting the curves $\Omega_p(l)$ and $n\Omega_H(l)$. So, in contrast to the point source model, the generation region of different bands are localized in different parts of the distributed source.

* However, when the induced scattering of plasma waves is essential, the fundamental radio emission (at the frequency close to Ω_p) may exceed the second harmonic radio emission (at the frequency (3.3)). In this case the observed zebra-pattern radio emission generated in the distributed source may appear to be polarized.

The distance between neighbouring levels of double resonance l_{n+1} and l_n is

$$\Delta l_n \approx \frac{L_H L_N}{nL_H - (n+1)L_N}, \tag{3.4}$$

where $L_H = H\,(\mathrm{d}H/\mathrm{d}l)^{-1}$ and $L_N = 2N\,(\mathrm{d}N/\mathrm{d}l)^{-1}$ are the characteristic scales of the magnetic field and electron density in the corona along the tube. For $L_H \ll L_N$ the value $\Delta l_n \approx L_H(n+1)^{-1}$ but for $L_H \gg L_N$ the distance $\Delta l_n \approx L_N/n$. For the zebra-pattern not to be 'diffused' and the dynamic spectrum to remain an oscillating character, the transverse dimensions of the flux tube are to be less than Δl_n (3.4).

The generation scheme (3.2)–(3.3) resembles the mechanism of the fine-structure generation in the type III bursts considered by Zheleznyakov and Zlotnik (1971). An essential difference is the following. Earlier the double plasma resonance resulted from the plasma wave absorption in the equilibrium coronal plasma (at the angles $\alpha \lesssim 1$). Now for waves propagating in the direction close to the transverse ($\alpha \approx \pi/2$) one, such an absorption becomes weak and the presence of nonequilibrium electrons causes their effective excitation.

Let us assume now that the energy of nonequilibrium particles in the flux tube is large enough for the cyclotron kinematic instability boundary λ_{cr} (I.3.17) to move into the region $\lambda_{\mathrm{cr}} < n$ situated from the left of the maxima of the curves $\omega(\lambda)$ in Figure I.2a. In the region of the normal dispersion the plasma wave generation will essentially depend on the ratio Ω_p/Ω_H. It follows from Figure I.6b that the increments increase sharply at $\Omega_p \approx n\Omega_H$. This implies that for the distributed source model the plasma wave energy will be higher in the layers situated near the levels of the double plasma resonance l_n (Figure 2). Then it is clear from Figure 2 that for arbitrary distributions $\Omega_p(l)$ and $\Omega_H(l)$, the frequencies (3.3), corresponding to the effective plasma waves and radio emission generation, are not equidistant. The nonequidistance will depend on the concrete distribution of $\Omega_p(l)$ and $\Omega_H(l)$ along the flux tube, the temporal change in this distribution causing the frequency drift of harmonic bands. The distance between radio emisson bands in the generation scheme differs from Ω_H. As follows from Figure 2 and relation (3.3), it is equal to

$$\Delta\omega = 2|\Omega_p(l_{n+1}) - \Omega_p(l_n)|\,. \tag{3.4}$$

The given difference may be represented in the form

$$\Delta\omega \approx \frac{2n\Omega_H L_H}{|nL_H - (n+1)L_N|}. \tag{3.5}$$

For $\Omega_H \ll \Omega_p$ (i.e. at $n \gg 1$) this formula takes on the form

$$\Delta\omega \approx \frac{2\Omega_H L_H}{|L_H - L_N|} \tag{3.6}$$

(cf. with the expression for $\Delta\omega$ (6) in the paper by Zheleznyakov and Zlotnik (1971)). Depending on the ratio L_N/L_H, the interval between neighbouring emission bands in the zebrapattern $\Delta\omega$ (3.6) varies from $2\Omega_H$ to $2\Omega_H L_H/L_N$. Under the condition $L_H \gg L_N$

(a slow change in the magnetic field),

$$\Delta\omega \approx 2\Omega_H ; \tag{3.7}$$

if $L_H \ll L_N$ (a fast change in the magnetic field), the interval is shortened up to*

$$\Delta\omega \approx 2\Omega_H L_H/L_N \ll 2\Omega_H . \tag{3.8}$$

The ratios (3.5) to (3.8) are to be taken into account in estimations of Ω_H and the magnetic field using the observed values of $\Delta\omega$ in the zebra-pattern. A confident conclusion on the value Ω_H according to the known $\Delta\omega$ in the distributed source model is impossible without estimating the ratio L_H/L_N. The latter is not necessary in the point source model where always $\Delta\omega \simeq \Omega_H$.

The extension of the effective generation region in the flux tube in the vicinity of l_n, corresponding to the double plasma resonance, depends on λ_{cr} (or on the energy of the nonequilibrium component; see the formula (I.3.17)) and on the coronal plasma parameters. For $v_e/v_T \sim 20$ and $\Omega_p/\Omega_H \sim 15$, as it is accepted in Figure I.6a, the range of values Ω_p/Ω_H in which there takes place the enhanced generation, occupies the substantial part of the band between the nearest gyrofrequency harmonics. It is true both for the frequency intervals of enhanced and moderate emission in the zebra-pattern and for the extension of the corresponding generation regions along the flux tube.

The minimum value of the nonequilibrium electron density, for which the zebra-structure generation in the magnetic tube starts, may be estimated under the condition $\gamma > \nu_{ef}$ (γ is the kinematic increment, ν_{ef} is the collisional number in the coronal plasma). It is seen from Figure I.6a that for the most favourable ratio Ω_h/Ω_H the increment $\gamma \approx \Omega_H N_e/N_0$ (for $v_e = 20 v_T$ and $\Omega_h \simeq 15\Omega_H$). Assuming that $\nu_{ef} \approx 35\ \mathrm{s}^{-1}$, $\Omega_H \sim 2\pi \times 15$ MHz and $N_0 \sim 5 \times 10^8\ \mathrm{cm}^{-3}$ we obtain that $N_e > 200$ el. cm^{-3}. This boundary for N_e is three orders lower than the corresponding estimations for tadpoles presented in Part II.

The latter circumstance is responsible for frequent appearance of the zebra-pattern emission which has no remarkable features typical of tadpoles. An ordinary character of the zebra-structure emission is also related to its primary generation in the distributed source, realized in the corona under less hard conditions than in the point source.

4. Conclusion

Part I of this paper deals with the cyclotron instability of the coronal plasma for Bernstein modes and plasma waves in a hybrid band. The results of investigations are used in Parts II and III to explain the features of such a fine structure of the solar radio emission as tadpoles and zebra-pattern. This explanation is essentially based on the effects of longitudinal wave excitation by nonrelativistic particles in the coro-

* One should bear in mind that when the fundamental emission prevails the second harmonic emission, factor 2 is to be omitted in (3.4)–(3.8).

na at the harmonics of the electron gyrofrequency. It is quite possible that these effects are rather essential also for generation of some other types of the fine structure of the solar radio emission.

Among the results obtained in Parts I–III the most important are:

(1) interpretation of the frequency spectrum of tadpoles as a result of relativistic and kinematic instability for the waves with anomalous dispersion (Bernstein modes);

(2) explanation of the pulsating excitation of the zebra-structure on 2 March 1970 taking into account the enhanced plasma wave excitation at the double plasma resonance;

(3) possibility of the zebra-structure generation in the distributed source where the emission bands occur at the levels of the double plasma resonance.

For a further development of the theory of those types of the fine structure which are related with the instabilities at the cyclotron harmonics, it is necessary:

(1) to study the nonlinear regime of generation of Bernstein modes and plasma waves in a hybrid band with taking into account the process of quasilinear relaxation of nonequilibrium particles and nonlinear wave transfer over the spectrum,

(2) to investigate conversion of longitudinal waves into the electromagnetic radiation due to combination scattering with allowance for the decay process of an electromagnetic wave.

This makes it possible to estimate the nonequilibrium electron density and the level of excited longitudinal waves necessary for the radio emission with the observed intensity. Also, the problem of the local source formation in a trap or in a flux tube and of the nonequilibrium particle production in the generation region is of great significance.

Note added in proof. By courtesy of Dr Kuijpers we have got acquainted with his thesis (Utrecht, 1975). It contains the same idea about the origin of zebra-structure as that given in the present paper for the distributed source model. However Kuijpers takes the hydrodynamic loss-cone instability that occurs if $N_e \gg 2\hbar s\beta^4 N_0$. For the velocity $v_e \sim 10^{10}$ cm s^{-1} ($\beta \sim 0.3$) taken by him and at the harmonic $s=5$ the above equality leads to $N_e \gg 0.4\, N_0$. In our variant the plasma wave instability is the kinetic cyclotron instability; the latter is realized when the hot electron density N_e is considerably less ($N_e \gtrsim 10^{-6}\, N_0$).

Acknowledgement

We are grateful to Dr V. V. Zaitsev for useful discussions.

References

Chiuderi, C., Giachetti, R., and Rosenberg, H.: 1973, *Solar Phys.* **33**, 225.

Elgarøy, Ø.: 1961, *Astrophysica Norvegica*, **7**, 123.

Rosenberg, H.: 1972, *Cosmic Plasma Physics*, ed. by K. Schindler, Plenum Press, New York and London, p. 191.

Slottje, C.: 1972a, *Proceedings of the 2nd Meeting of the CESRA, 1971*, (Trieste), p. 88.

Slottje, C.: 1972b, *Solar Phys.* **25**, 210.
Zaitsev, V. V. and Stepanov, A. V.: 1974, *Soviet Solar Data* **11**, 71.
Zaitsev, V. V. and Stepanov, A. V.: 1975, *Astron. Astrophys.*, in press.
Zheleznyakov, V. V. and Zlotnik, E. Ya.: 1971, *Solar Phys.* **20**, 85.
Zheleznyakov, V. V. and Zlotnik, E. Ya.: 1975a, *Solar Phys.* **43**, 431.
Zheleznyakov, V. V. and Zlotnik, E. Ya.: 1975b, *Solar Phys.*, this issue, p. 447.